doi:10.1111/evo.12575

Modular color evolution facilitated by a complex nanostructure in birds

Chad M. Eliason,[1,2,3] Rafael Maia,[1] and Matthew D. Shawkey[1]

[1]*Department of Biology and Integrated Bioscience Program, The University of Akron, Akron, Ohio 44325*

[2]*Current address: Department of Integrative Biology, University of Texas, Austin, Texas 78712*

[3]*E-mail: chad_eliason@utexas.edu*

Received July 23, 2014

Accepted November 11, 2014

The way in which a complex trait varies, and thus evolves, is critically affected by the independence, or modularity, of its subunits. How modular designs facilitate phenotypic diversification is well studied in nonornamental (e.g., cichlid jaws), but not ornamental traits. Diverse feather colors in birds are produced by light absorption by pigments and/or light scattering by nanostructures. Such structural colors are deterministically related to the nanostructures that produce them and are therefore excellent systems to study modularity and diversity of ornamental traits. Elucidating if and how these nanostructures facilitate color diversity relies on understanding how nanostructural traits covary, and how these traits map to color. Both of these remain unknown in an evolutionary context. Most dabbling ducks (Anatidae) have a conspicuous wing patch with iridescent color caused by a two-dimensional photonic crystal of small (100–200 nm) melanosomes. Here, we ask how this complex nanostructure affects modularity of color attributes. Using a combination of electron microscopy, spectrophotometry, and comparative methods, we show that nanostructural complexity causes functional decoupling and enables independent evolution of different color traits. These results demonstrate that color diversity is facilitated by how nanostructures function and may explain why some birds are more color-diverse than others.

KEY WORDS: **Evolvability, iridescence, Ornstein–Uhlenbeck model, sexual selection.**

Complex morphological traits consisting of multiple subunits are common in nature and have evolved to serve diverse functions, from competition for mates (Emlen et al. 2005), to prey capture (Schaeffer and Rosen 1961) and flight (Kingsolver and Koehl 1994; Prum and Dyck 2003). Selection pressures can only act upon the standing phenotypic variation of a trait, which in turn depends on how independent (modular) its component parts are genetically, developmentally, or functionally (Wagner et al. 2007; Klingenberg 2008; Pigliucci 2008). With complex traits that perform physiological or biomechanical functions, selection acts on function or performance rather than directly on morphology, and therefore the relationship between form and function is crucial to understanding the morphological response to selection (Arnold 1983; Walker 2007). Consequently, innovations in how traits function can promote phenotypic diversity (Wainwright 2007). For example, the evolution of an additional pharyngeal jaw in cichlids from a simpler ancestral form with only a single oral jaw (Schaeffer and Rosen 1961) permitted different parts of the feeding apparatus to perform separate functions (prey capture and processing), thereby facilitating greater phenotypic diversity (i.e., more combinations in the shapes and sizes of the two jaws; Hulsey et al. 2006).

Changes in form–function relationships can increase morphological diversity in biomechanical and ecological traits (Alfaro et al. 2005; Stayton 2006; Wainwright 2007), but whether this holds true in ornamental traits is less understood (Ord et al. 2013; Maia et al. 2013b). Ornamental traits are often more diverse than ecological traits (Andersson 1994; Emlen et al. 2005), potentially because of the increased strength and constancy of sexual selection compared to natural selection (Hoekstra et al. 2001) or the greater potential for rapid divergence by a runaway process of coevolution between trait and preference (Prum 2010). Regardless of the strength and nature of sexual selection, evolutionary change in complex signaling phenotypes

EVOLUTION
INTERNATIONAL JOURNAL OF ORGANIC EVOLUTION

will ultimately depend on intrinsic features like genetic covariation among subunits (Chenoweth et al. 2010) or biomechanical limitations on signal production (Podos 1997; Ord et al. 2013). Therefore, elucidating the proximate bases of ornamental traits is crucial in understanding how they can diversify.

Plumage colors in birds are diverse ornamental traits involved in intra- and intersexual selection (Andersson 1994). Birds have two nonexclusive ways of producing feather colors: deposition of pigments that selectively absorb certain wavelengths of light (pigment-based colors) and organization of feather materials into nanostructures that selectively scatter certain wavelengths of light (structural colors). Color itself is a multidimensional trait commonly described by three optical parameters that summarize how light is reflected across a visible range of wavelengths. In general, brightness is a measure of how much light is reflected from a surface, hue is a measure of where in the avian visible spectrum reflectance is highest (e.g., blue or red wavelengths), and saturation describes the specificity of the reflection (i.e., over how narrow a range of wavelengths reflectance occurs). Depending on the mechanisms responsible for producing a color, these three parameters may vary independently (modular) or be strongly linked (integrated). For example, yellow feather colors in great tits (*Parus major*) are produced by lutein pigments that absorb light maximally at 450 nm (blue-green wavelengths). Increasing the concentration of lutein results in correlated changes in brightness, hue, and saturation (Andersson and Prager 2006). Therefore, these color variables are functionally coupled and have fewer unique combinations of color variables owing to this common mechanistic basis.

Structural colors are intrinsically linked to the nanostructural characteristics of the underlying morphology, such that variation in color attributes can be mapped to variations in the morphology of the color-producing nanostructure. Based on the deterministic association between color and the components that produce it, an increase in the number of tunable nanostructural parameters may increase the number of independent optical parameters (Holzman et al. 2011). Structural colors are therefore an exemplary system for studying how innovations in the way traits function can facilitate color diversity. However, elucidating the mechanisms by which nanostructural templates facilitate color diversity relies on an understanding of how complexity enables the independent evolution of different nanostructural traits (modularity), and how these nanostructural modules map to color attributes, both of which remain unknown in an evolutionary context.

Most species of dabbling ducks (tribe *Anatini*) have a conspicuous patch of colorful plumage, called the speculum, in their wings that is often monomorphic (found in both males and females) and iridescent. These gaudy plumage patches vary considerably in color (Eliason and Shawkey 2012) and in some species are sexually selected (Omland 1996). The considerable interspecific variation in color is caused by nanoscale changes in the underlying nanostructure: a two-dimensional hexagonal photonic crystal formed of 100–200 nm melanosomes (Eliason and Shawkey 2012). Compared to simple structures like keratin or melanin thin films, nanostructures in ducks are complex, with multiple parameters (e.g., the size and spacing of melanosomes) determining the structural form (Eliason and Shawkey 2012). These multiple subunits may control different aspects of speculum color, and the degree to which they are functionally and evolutionarily independent may dictate how the colorspace can be explored during diversification. Here, we ask whether functional decoupling among nanostructural traits facilitates color diversification. Specifically, we tested the following three predictions: (i) color variation is explained by variation in nanostructural traits, (ii) traits that map to specific color properties (functional modules) evolve independently and at different rates, and (iii) rates of color evolution parallel those in the nanostructural traits that produce them.

Methods

SAMPLING SPECIES AND RECONSTRUCTING PHYLOGENETIC RELATIONSHIPS

Of the 54 recognized species in the *Anatini* subfamily (Gill and Donsker 2014), we obtained samples from the 44 with DNA sequences available from GenBank for molecular phylogenetic reconstruction. We obtained nanostructural and color measurements from feathers of specimens at the Field Museum of Natural History and the University of Michigan Museum of Zoology (see Supporting Information Table S1 for details). We sampled all dabbling duck species except for four that had noniridescent wing patches (*Tachyeres pteneres*, *Anas georgica*, *A. sibilatrix*, and *A. strepera*) and two that had no suitable specimens at the collections (*A. bernieri* and *A. smithii*). In total, our dataset included phylogenetic and phenotypic data for 38 species.

We estimated a time-calibrated phylogeny for dabbling ducks using published sequences for two mitochondrial genes, cytochrome b oxidase, and NADH dehydrogenase (Johnson and Sorenson 1999; Gonzalez et al. 2009), and an uncorrelated relaxed clock algorithm implemented in the program BEAST 1.7.4 (Drummond and Rambaut 2007). We used available fossil data and exponential priors to place constraints on the root age and divergence times for six internal nodes (see Supporting Information Table S2). We used a starting tree estimated in MrBayes version 3.1.2 (Huelsenbeck and Ronquist 2001) and ran five separate analyses in BEAST for 10 million generations each, sampling every 10,000 generations, and checked that these independent analyses reached stationarity at the same region of parameter space using Tracer version 1.5. For comparative analyses, we obtained a maximum clade credibility (MCC) summary tree of a sample of 500

trees from the posterior distribution to incorporate phylogenetic uncertainty in the evolutionary model estimates. All trees were made time-proportional by scaling to a total depth of one.

MEASURING SPECTRAL REFLECTANCE AND QUANTIFYING COLOR

To quantify color, we measured spectral reflectance of intact wing patches for wavelengths between 300 and 700 nm using a spectrophotometer and Xenon light source (Avantes Inc., Broomfield, CO). Iridescent colors are defined by their capacity to vary with angle. Therefore, to control for this effect when quantifying interspecific variation, we measured all spectra at coincident normal geometry (with the bifurcated light and measurement probes perpendicular to the feather surface). We took three measurements from one of the wings of 1–5 males per species, completely removing the probe between measurements and haphazardly selecting a different spot on the speculum. After measuring reflectance, we smoothed spectra with local regression using the loess function in R version 3.0.2 (R Development Core Team 2013) to minimize electrical noise from the spectrophotometer and thus increase the accuracy of color variable calculation.

From the processed spectra, we characterized speculum color based on three attributes from the reflectance spectra. First, we determined hue as the wavelength of the primary reflectance peak. Second, we quantified saturation as the half-width of the main reflectance peak at 50% of peak reflectance. Third, we measured brightness as the maximum reflectance of the main peak. Because brightness is highly sensitive to variation in alignment of the spectrophotometer with respect to the orientation of feather structures (Meadows et al. 2011), we retained the brightest of the three spectra per bird for further analyses. These three color variables were chosen because they allow for direct comparison with optical model predictions for photonic crystals (Joannopoulos et al. 2008; Eliason and Shawkey 2012). All color analyses were performed in the R package pavo version 0.5–1 (Maia et al. 2013a).

QUANTIFYING COLOR-PRODUCING NANOSTRUCTURE

The structural features of photonic crystals responsible for producing color in visible wavelengths are at the nanoscale, and therefore we used transmission electron microscopy (TEM) micrographs of barbule cross-sections to quantify relevant morphological parameters (see Supporting Information for TEM protocol). We then used ImageJ software (Abràmoff et al. 2004) to measure (i) the diameter of melanosomes, (ii) the separation between melanosomes, and (iii) the number of layers in a melanosome stack measured perpendicular to the barbule surface. These parameters are sufficient to describe and model color production by two-dimensional photonic crystals and have been demonstrated to control color variation in duck specula (Eliason and Shawkey 2012). Although the thickness of the keratin layer at the outer edge of barbules (cortex) could affect color, the main reflectance peak is controlled primarily by the underlying photonic crystal (Eliason and Shawkey 2012), thus we did not include cortex thickness in our analyses.

We took measurements from 10 haphazardly chosen regions within 1–3 barbules per species to account for potential nonindependence in the sizes of adjacent melanosomes. We natural log-transformed all nanostructural and color variables and then computed species means prior to statistical analyses (data are available on Dryad; http://www.datadryad.org/). This transformation allowed us to compare evolutionary rates among traits measured in different ways or with different units (e.g., percent brightness and nanometer diameter) by representing variation in proportional change in units of e (2.7) (Gingerich 2009; Adams 2013).

MODELING CHARACTER EVOLUTION

To explore the evolutionary mode of color and nanostructural traits, we fit multivariate Brownian motion (BM) and Ornstein–Uhlenbeck (OU) models of character evolution separately to both sets of traits using maximum likelihood in the R package ouch (Butler and King 2004). We further tested if multivariate OU models considering correlations between traits within a set of traits (i.e., among color variables and among nanostructural variables separately) outperformed univariate OU models (where traits were considered to be uncorrelated).

We tested the power to differentiate between BM and OU models, as well as univariate and multivariate OU models, using a phylogenetic Monte Carlo (pmc) approach (Boettiger et al. 2012). Briefly, we estimated parameters for each posterior tree in ouch, then randomly sampled one of these trees (and its respective estimates) to simulate traits evolving along that phylogeny under both the null and test models. We then reestimated parameters for the simulated datasets under each model and calculated the deviance as $\delta = 2 * (\log\mathcal{L}_{\text{null}} - \log\mathcal{L}_{\text{test}})$. We repeated this simulation process 1000 times to obtain deviance distributions considering model and phylogenetic uncertainty. Comparing the overlap in these distributions gives the power to distinguish between the two models, and comparing the observed deviance to the null distribution gives the probability of observing a value equal to or more extreme than that obtained from data simulated under the null model (Boettiger et al. 2012).

LINKING FORM TO FUNCTION

To test our hypothesis that the form-function relationship biases the tempo and mode of color evolution, we quantified the relationship between feather nanostructure and color using phylogenetic generalized least squares (PGLS) multiple regression. We

only considered a full additive model based on expectations from physics (Joannopoulous 2008) and previous optical modeling results in this group (Eliason and Shawkey 2012). We accounted for phylogenetic effects on trait covariation under an OU process using the corMartins function in the ape package (Hansen 1997). Phylogenetic effects are accounted for in the OU model by the phylogenetic half-life, which is inversely proportional to twice the attraction parameter α (Hansen 1997), and therefore was allowed to vary depending on the maximum likelihood estimate of α. To account for phylogenetic uncertainty in parameter estimates, we ran PGLS models for each color variable on all 500 posterior trees, and retained parameter estimates as well as their standard deviations. The sum of the among-tree and average within-tree variance in parameter estimates was then used to statistically test for the effect of the different response variables in the models. PGLS analyses were conducted in R version 3.1.0 using the packages nlme version 3.1–117 and ape version 3.1.3 (Paradis et al. 2004). We used multivariate Q–Q plots to assess normality and transformed variables when necessary (see Supporting Information for details). Variables were centered and scaled by their standard deviations prior to analyses in order to obtain standardized regression coefficients (Schielzeth 2010). To assess model fit, we calculated pseudo-R^2 following (Paradis 2012) and computed mean and 95% confidence intervals across the tree block.

CALCULATING EVOLUTIONARY RATES AND MODULARITY

Evolutionary rates describe how quickly variation accumulates over a given period of time (Martins 1994). Under a Brownian motion model, variation increases linearly as a function of σ^2 and time. By contrast, under an OU model, the time-variance relationship is nonlinear: variation in traits increases at first, but as a result of the action of the attraction parameter α, the rate of variance accumulation slows down, and will eventually reach a plateau and be constant over time (Hunt 2012; Slater 2013). Evolutionarily, this is often interpreted as a balancing out of variance-generating mechanisms (e.g., drift, mutation) and variance-restraining forces (e.g., selection, developmental constraints; Hansen 1997; Martins et al. 2002). For this reason, rates of trait evolution cannot be inferred from σ^2 alone if the model that best describes trait evolution is any other than a Brownian motion model (Martins 1994; Slater 2013). However, if we interpret rates of evolution as the average rate of variance accumulated over the evolutionary history of a lineage from its root ancestor up to the present time, we can estimate rates from an OU process as a function of σ^2, α, and time. To do this, we used published equations (Hansen and Martins 1996; Bartoszek et al. 2012) to calculate the evolutionary variance-covariance matrix **V** under an OU process (equation B.8 in Bartoszek et al. 2012). These equations do not assume stationarity of the OU process, and thus we used the total evolutionary time from the MRCA to the tips as our unit of time. We then used **V** to (i) compare the rates at which different traits have evolved (diagonals of V, comparable to the rate metric ω in Hunt 2012) and (ii) test whether different pairs of traits evolve independently or in a correlated fashion (off-diagonals of **V**).

To calculate confidence intervals for elements of **V**, we used a parametric bootstrap approach to simulate evolution under the best fitting multivariate OU model, each time sampling a tree at random from the posterior distribution. Rarefaction of variance analyses showed that approximately 5000 simulations captured the variation in estimates for both diagonal and off-diagonal components of **V** (Supporting Information Figs. S1 and S2), therefore we used 5000 simulations in all subsequent analyses (see Supporting Information for details). To test for correlated evolution (i.e., lack of modularity), we evaluated whether the 95% confidence intervals of trait covariance estimates obtained from the parametric bootstrap routine overlapped zero. To test if traits evolved as interdependent modules or if differences in evolutionary rates among them exist, we calculated pairwise contrasts in evolutionary rates for all pairwise combinations among color and nanostructural traits separately. We then assessed significance by examining whether the 95% confidence intervals of these contrasts overlapped zero after applying sequential Bonferroni correction to account for multiple tests (Holm 1979).

MEASUREMENT ERROR AND OUTLIER SENSITIVITY

Comparisons of evolutionary rates among different phenotypic traits are prone to measurement error (Harmon and Losos 2005; Ives et al. 2007; Adams 2013). Examining barbule nanostructure for many individuals of all species is unfeasible. Therefore, following Harmon et al. (2010), we used an estimate of intraspecific variation in color and nanostructural traits for one of the species (mallard, *Anas platyrhynchos*) that had been sampled densely for a separate study, and then repeated all analyses described above. Although this assumes similar measurement error across all species, calculating rates with and without error allowed us to evaluate the relative sensitivity of different traits to measurement error, and therefore determine whether our results are robust (e.g., see Harmon et al. 2010).

Bivariate plots of nanostructural and color variables revealed two potential outlier species: *Anas aucklandica*, with a very broad reflectance peak (see Supporting Information Fig. S3) and *A. rubripes,* with the smallest melanosome diameter and spacing (see Supporting Information Fig. S4). To assess whether these species affected our results, we pruned them from the phylogenies and reran all analyses (see Supporting Information).

Results

PHYLOGENY

All chains reached stationarity around the same optimal likelihood value and all parameters had effective sample sizes (ESS) greater than 116. The MCC tree was very similar to Johnson and Sorenson (1999) and recapitulated most of the topology of Gonzalez et al. (2009), with only slight differences (see Supporting Information Fig. S5).

COLOR VARIATION IS EXPLAINED BY VARIATION IN NANOSTRUCTURAL TRAITS

All duck species with iridescent speculum feathers had melanosomes organized in hexagonal arrays characteristic of the two-dimensional photonic crystal previously described (Eliason and Shawkey 2012). Melanosome diameter ranged from 90 to 180 nm, spacing between adjacent melanosomes varied from 18 to 87 nm, and the number of layers at the surface of barbules ranged from 4 to 8. Hue spanned from blue (463 nm) to red (647 nm), saturation ranged from 32 to 69 nm, and brightness varied from 5 to 70% reflectance. Species with larger melanosomes had redder (PGLS: $\beta = 0.36 \pm 0.18$, $t = 2.07$, $P = 0.045$, df $= 34$, $R^2 = 0.27$ [0.15, 0.74]; Fig. 1A) and less saturated colors ($\beta = -0.50 \pm 0.18$, $t = -2.77$, $P = 0.0089$, df $= 34$, $R^2 = 0.38$ [0.19, 0.83]; Fig. 1B), whereas species with more open hexagonal arrays—that is, greater distance between its melanosomes—had brighter colors ($\beta = 0.43 \pm 0.16$, $t = 2.69$, $P = 0.011$, df $= 34$, $R^2 = 0.24$ [0.15, 0.56]; Fig. 1C). Melanosome diameter did not significantly influence brightness ($\beta = -0.35 \pm 0.20$, $t = -1.77$, $P = 0.085$). Melanosome spacing did not significantly predict hue ($\beta = -0.064 \pm 0.15$, $t = -0.42$, $P = 0.67$) or saturation ($\beta = 0.22 \pm -0.16$, $t = 1.37$, $P = 0.18$). The number of melanosome layers was not a significant predictor of any color variable.

COLOR AND NANOSTRUCTURAL TRAITS EVOLVE BY A MULTIVARIATE O–U PROCESS

The multivariate OU model was strongly preferred over the BM model for both color and nanostructural traits (both $P < 0.001$). Phylogenetic Monte Carlo simulations showed that there was adequate power to tell these models apart, as there was no overlap in the distribution of deviances obtained by comparing models from traits simulated under BM or OU models (see Supporting Information Fig. S6A, B). We also found strong support for the multivariate over the univariate OU model (i.e., off-diagonal elements of σ^2 and α set equal to zero) for both suites of traits (both $P < 0.001$; power = 99.3% and 98.0% for color and nanostructural traits, respectively; see Supporting Information Fig. S6C, D).

FUNCTIONAL MODULES EVOLVE INDEPENDENTLY AND AT DIFFERENT RATES

Under the multivariate OU model, melanosome spacing was positively correlated with melanosome diameter and the number of melanosome layers (Fig. 2A). Saturation was positively correlated with hue and negatively correlated with brightness, but brightness and hue were not significantly correlated (Fig. 2B). We found a similar pattern for PGLS predicted color variables (see Supporting Information results, Fig. S9A).

Melanosome spacing evolved significantly faster (~5.5X) than the size of melanosomes or the number of layers, with no significant differences between the rates of the latter two (ratio = 1.9; Fig. 3A). All color traits had significantly different evolutionary rates, with brightness evolving significantly faster than hue (~73X) and saturation (~17X), and saturation evolving ~4X faster than hue (Fig. 3B). We obtained a similar result for color variables predicted using the PGLS model (Supporting Information Fig. S9B). Both color and nanostructure rate comparisons were unaffected by the removal of outliers (see Supporting Information).

EFFECTS OF MEASUREMENT ERROR AND OUTLIERS

PGLS results were generally robust to potential outliers, as only the hue-diameter relationship became marginally nonsignificant without *Anas aucklandica* in the analysis ($P = 0.06$). All traits had lower evolutionary rates when incorporating measurement error, but the pattern of rate differences among traits was not affected (see Supporting Information Fig. S7). Correlations among nanostructural traits were sensitive to measurement error (diameter-spacing becoming significantly positive; Supporting Information Fig. S8A) and whether *A. rubripes* was included in the analysis (diameter-spacing relationship becoming nonsignificant). Correlations among color variables remained similar with incorporating measurement error (Supporting Information Fig. S8B).

Discussion

How modularity affects phenotypic evolution is a critical question in biology (Schwenk et al. 2009). In this study, we densely sampled nanoscale feather morphologies within an avian clade to test how the functional architecture of a complex trait relates to macroevolutionary patterns of trait diversity. To do this, we first explored the relationship between form and function and whether this relationship results in functional decoupling among nanostructural traits. Melanosome diameter was positively associated with hue and negatively associated with saturation, while spacing between melanosomes was positively associated with brightness. Thus, our evolutionary regressions suggest that melanosome

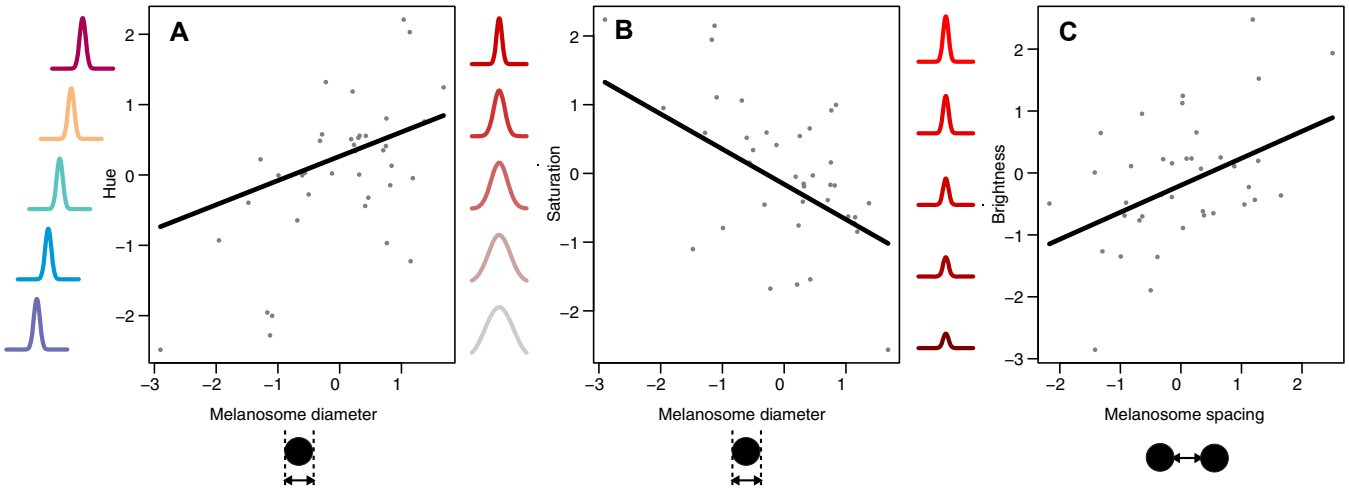

Figure 1. Phylogenetic generalized least squares (PGLS) multiple regression results for the maximum clade credibility (MCC) tree in dabbling ducks. Plots show conditional plots of color variables hue (A), saturation (B) and brightness (C) versus their nanostructural predictors. Relationships between variables were calculated by holding all other variables in multiple regressions at their median values using the visreg package (version 2.0.5) in R. Lines are linear fits. Schematics along *y*-axes illustrate relevant variation in the shape of reflectance spectra (color online).

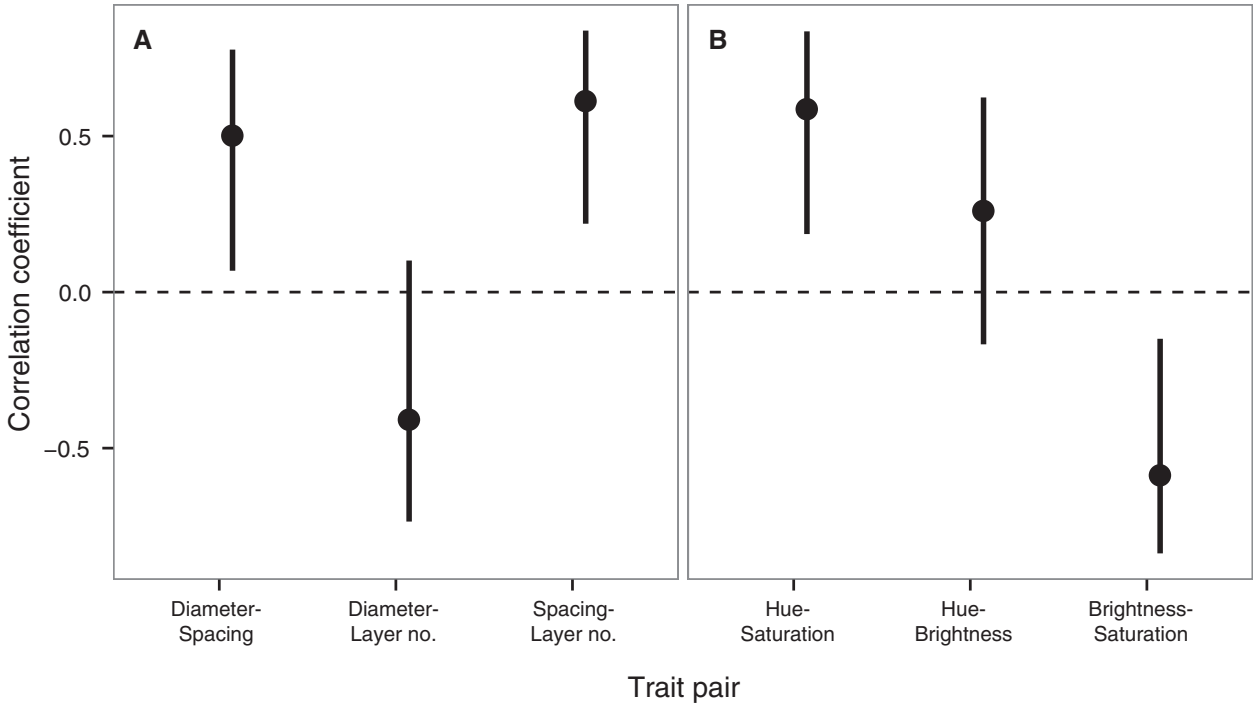

Figure 2. Evolutionary correlations among pairs of nanostrutural (A) and color traits (B). Points show mean rate and line segments are 95% confidence intervals. Results are for analyses incorporating measurement error.

diameter and spacing are, at least in part, functionally independent (i.e., they contribute to separate color attributes). Next, we addressed the consequences of this functional decoupling for the patterns and pace of color evolution. We found that decoupled color traits evolve independently and at different rates, and that correlated changes in color stem from a common mechanistic basis rather than strong covariation among morphological traits. For example, the near-zero correlation between hue and brightness suggests that functional complexity eliminates trade-offs between these optical traits (Holzman et al. 2011). By contrast, hue and saturation have evolved in a correlated fashion and at similar rates, and this integration may arise because of a common morphological basis (melanosome diameter). Taken together, these findings show that the way a nanostructure functions can affect its

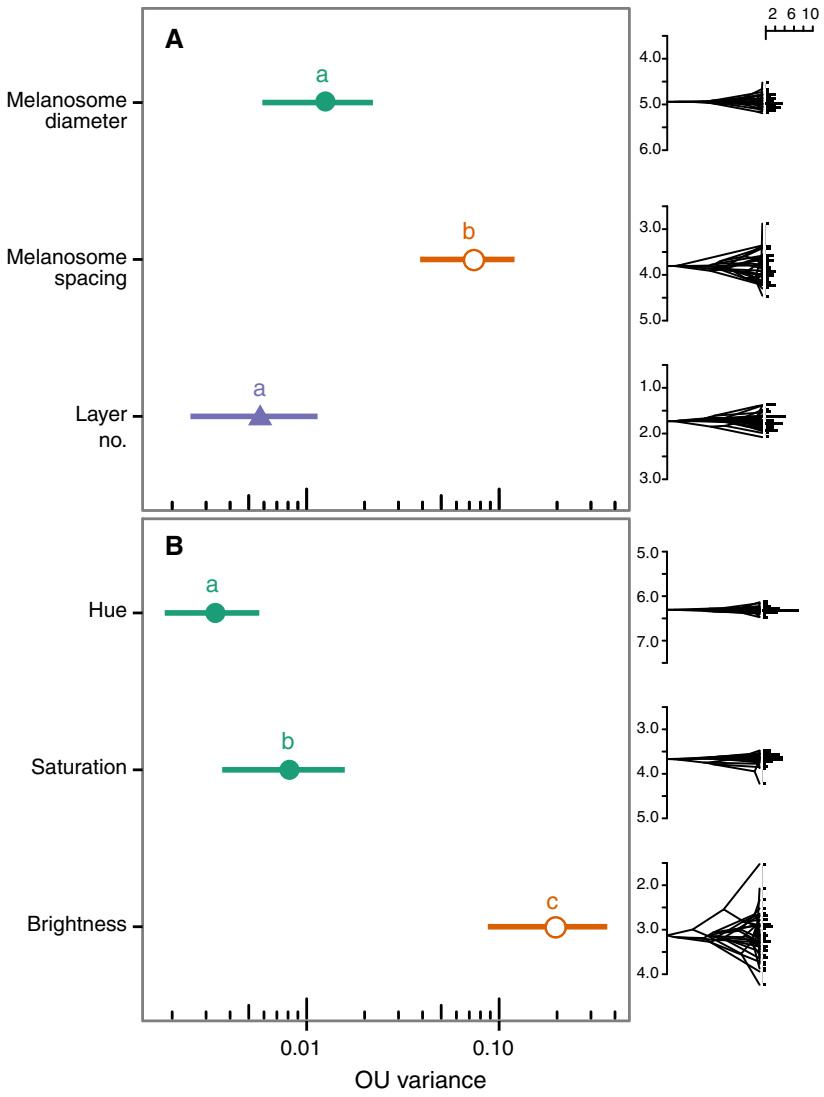

Figure 3. **Phenotypic divergence rates for different nanostructural (A) and optical traits (B). Points show mean evolutionary rates and 95% confidence intervals (horizontal lines) for analyses incorporating measurement error (note log-10 scale of *x*-axis). Similar symbols (and colors online) indicate functionally related traits inferred from PGLS analyses. Different letters indicate significantly different rates within groups of nanostructural and color traits (pairwise differences, intervals corrected for multiple comparisons with sequential Bonferroni tests; Holm 1979). "Traitgrams" (right outsets) illustrate relationship between time (*x*-axis) and evolutionary change in natural log-transformed trait values (*y*-axis), with histograms of tip values drawn at right. All *y*-axes have the same range in natural log units for easier comparison of accumulation of variation in different traits.**

evolution, and therefore they provide a mechanism for explaining why clades with more complex nanostructures evolve more diverse colors (Maia et al. 2013b).

FUNCTIONAL MODULARITY ENHANCES COLOR EVOLVABILITY

Modularity in the form-function mapping of two-dimensional photonic crystals in duck specula strongly affects their evolvability. These plumage traits may be involved in mate choice in species like northern pintails *Anas acuta*, where females were shown to prefer males with more iridescence in their wings (Sorenson and Derrickson 1994), or in mallards (*Anas platyrhynchos*), where the quality of wing patches determined seasonal pairing success (Omland 1996). Iridescent colors have also been suggested be condition-dependent in some species of ducks (Legagneux et al. 2010), highlighting their potential as honest visual signals. Despite rampant sexual dichromatism in overall body plumage within Anatidae (Omland 1997; Figuerola and Green 2000), many species have monochromatic wing patches (Madge and Burn 1988), suggesting potentially weak intersexual selection (Badyaev and Hill 2003). Whether and how these visual signals play a role in mate choice, intrasexual competition, or

species recognition remains a fertile area for future research. Nonetheless, our study shows that, whatever the selective forces acting on these colors, the intricacies of the structure underlying iridescent signals results in both the integration and modularity of color properties (Fig. 2, Supporting Information Fig. S9A), thus dictating how these color traits can evolve to explore the available color gamut that this flexible template provides (Fig. 3, Supporting Information S9B).

NANOSTRUCTURAL PREDICTORS OF COLOR

Interestingly, the number of melanosome layers was not a significant predictor of any color variable. A higher number of repeating layers should enhance brightness due to an additive coherent interference effect (Kinoshita 2008). However, estimates of intraspecific and interspecific variation in layer number were in the same range (Supporting Information Table S3). Number of layers is likely to be a developmentally plastic trait, controlled simply by the amount of melanin deposited in barbules during feather ontogeny (Maia et al. 2012). Moreover, it is functionally bounded on both extremes of its distribution, as at least two layers are needed for a hexagonally arranged photonic crystal, and because little light is reflected from more basal layers due to strong absorption. Therefore, while this trait likely affects brightness (Kinoshita 2008), it may play a minor role in explaining interspecific variation in color (Xiao et al. 2014) and is therefore unlikely to be a major axis of macroevolutionary variation.

The weak negative relationship between diameter and brightness is expected from optical theory, as larger melanosomes should produce broad reflectance peaks and bright colors (Eliason and Shawkey 2012). Thus, the observed significant correlation between brightness and saturation might stem from a common morphological basis. Another possible explanation for the correlation could be that more disordered melanosomes cause both duller colors and broader reflectance peaks. However, we did not find a significant relationship between the coefficient of variation in melanosome size, a measure of disorder (Rengarajan et al. 2005), and any color variables (see Supporting Information).

COMPLEXITY AND COLOR VARIABILITY

Complex traits with more parts have more potential for phenotypic variation. One of the most common nanostructures in birds is a thin film of keratin layered over packed, rod-shaped melanosomes (Durrer 1977). Since melanin absorbs light strongly across the entire human and avian visible spectrum, and assuming such optical properties are conserved among species, the only way that this structural template can produce different colors is through variation in the thickness of the keratin cortex. Therefore, this structure results in a single major axis of variation in color, with hue and saturation variation tracking cortex thickness (Doucet et al. 2006; Shawkey et al. 2006, also see Orfanidis 2008 Fig. 5.5.1 for optical background) and brightness being constrained by the lack of independent, tunable nanostructural components (see eq. 5.4.6 in Orfanidis 2008). Our results show that modifications to this nanostructural template open up the possibility for additional axes of nanostructural variation (melanosome diameter and spacing) with direct consequences for color diversity. Furthermore, iridescent color is itself a dynamic trait that varies with viewing angle (Newton 1704). Further research on the proximate bases of iridescence per se may shed light on the biological function and selective pressures of these complex visual signals.

STRUCTURAL TRAITS EVOLVE FASTER THAN MORPHOLOGICAL TRAITS

We found that brightness evolved faster than hue, and that this pattern emerges because structural aspects of the photonic crystal (i.e., the arrangement of its components) diverge faster than the morphological "building blocks" comprising it. This pattern is likely caused by differences in the evolutionary variances of traits rather than contrasting selection or constraint (Supporting Information Fig. S10). However, the question of why structural traits diverge faster than morphological ones remains unanswered. Melanosome synthesis and deposition are complex processes involving a number of genes (reviewed in Marks and Seabra 2001). Compared to melanosome morphology, the organization of melanosomes is likely sensitive to additional ontogenetic factors like cellular homeostasis and rates of melanosome deposition and keratin polymerization during barbule development (Dufresne et al. 2009; Maia et al. 2012). Traits produced by more complex developmental processes may evolve more quickly due to their increased evolutionary degrees of freedom (Wund 2012). Even though, at larger scales, melanosome morphology shows considerable morphological variation (Li et al. 2012), melanosome morphology is usually highly conserved among closely-related species (Greenewalt et al. 1960; Durrer 1977; Shawkey et al. 2006), with very few exceptions (Maia et al. 2013b). The melanosomes responsible for the two-dimensional crystal structure found in ducks (Eliason and Shawkey 2012) are among the thinnest and longest found in birds (Li et al. 2012). This aspect of their morphology might be critical in allowing the formation of these patterns, which might explain their rarity among birds (Prum 2006). The limitations on melanosome morphology needed to produce a functional two-dimensional hexagonal structure may further limit the range of functional morphologies, and thus the rate of evolution of melanosome shape.

IMPLICATIONS FOR COLOR DIVERSIFICATION

The macroevolutionary consequences of sexual selection on ornamental diversity and speciation have long been central to evolutionary studies, both from an empirical and a theoretical

standpoint (West-Eberhard 1983; Ritchie 2007). However, very few studies have explored how the proximate mechanisms of functional traits (like color) influence their evolution (Emlen et al. 2007; Maia et al. 2013b; Ord et al. 2013). With colorful ornaments, different spectral variables may convey unique messages to other individuals. For example, variation in brightness in poison dart frogs is perceived by conspecifics but not predators (Crothers and Cummings 2013). Moreover, there is considerable variation in the spectral targets of selection in birds (e.g., hue or brightness), both within and among species with different color-producing mechanisms (reviewed in Hill 2006). As we demonstrate in this study, the capacity of different color traits to diverge independently may facilitate divergence among populations depending on how strong and divergent are female preferences (Rodríguez et al. 2013). Coupling our approach of studying proximate mechanisms of coloration with further studies on the strength and nature of sexual selection within populations will elucidate whether patterns of covariation in color traits (e.g., Safran and Mcgraw 2004) are due to common mechanisms or correlated selection, and ultimately help to link microevolutionary processes with macroevolutionary patterns in color.

ACKNOWLEDGMENTS

We thank Liliana D'Alba and Branislav Igic for comments on an earlier version of this manuscript; Aaron King and Krzysztof Bartoszek for their comments and assistance with implementing multivariate comparative methods; and Janet Hinshaw at the University of Michigan Museum of Zoology and David Willard of the Field Museum of Natural History for allowing us access to their bird skin collections to sample feathers for spectral and electron microscope analyses. The authors declare no competing financial interests. This work was supported by AFOSR grant FA9550-09-1-0159, NSF grant EAR-1251895, HFSP grant RGY0083 (all to M.D.S.), and NSF grant Grant DEB-1210630 (to R.M.).

DATA ARCHIVING

The doi for our data is 10.5061/dryad.4387q.

LITERATURE CITED

Abràmoff, M. D., P. J. Magalhães, and S. J. Ram. 2004. Image processing with ImageJ. Biophotonics Int. 11:36–42.

Adams, D. C. 2013. Comparing evolutionary rates for different phenotypic traits on a phylogeny using likelihood. Syst. Biol. 62:181–192.

Alfaro, M. E., D. I. Bolnick, and P. C. Wainwright. 2005. Evolutionary consequences of many-to-one mapping of jaw morphology to mechanics in Labrid fishes. Am. Nat. 165:E140–E154.

Andersson, M. 1994. Sexual selection. Princeton Univ. Press, Princeton, NJ.

Andersson, S., and M. Prager. 2006. Quantifying colors. Pp. 41–89 *in* K. J. McGraw and G. E. Hill, eds. Bird coloration: volume I. Harvard Univ. Press, Cambridge, MA.

Arnold, S. J. 1983. Morphology, performance and fitness. Integr. Comp. Biol. 23:347–361.

Badyaev, A. V., and G. E. Hill. 2003. Avian sexual dichromatism in relation to phylogeny and ecology. Annu. Rev. Ecol. Evol. Syst. 34:27–49.

Bartoszek, K., J. Pienaar, P. Mostad, S. Andersson, and T. F. Hansen. 2012. Journal of theoretical biology. J. Theor. Biol. 314:204–215.

Boettiger, C. C., G. G. Coop, and P. P. Ralph. 2012. Is your phylogeny informative? Measuring the power of comparative methods. Evolution 66:2240–2251.

Butler, M., and A. King. 2004. Phylogenetic comparative analysis: a modeling approach for adaptive evolution. Am. Nat. 164:683–695.

Chenoweth, S. F., H. D. Rundle, and M. W. Blows. 2010. The contribution of selection and genetic constraints to phenotypic divergence. Am. Nat. 175:186–196.

Crothers, L. R., and M. E. Cummings. 2013. Warning signal brightness variation: sexual selection may work under the radar of natural selection in populations of a polytypic poison frog. Am. Nat. 181:E116–E124.

Doucet, S., M. D. Shawkey, G. E. Hill, and R. Montgomerie. 2006. Iridescent plumage in satin bowerbirds: structure, mechanisms and nanostructural predictors of individual variation in colour. J. Exp. Biol. 209:380–390.

Drummond, A. J., and A. Rambaut. 2007. BEAST: Bayesian evolutionary analysis by sampling trees. BMC Evol. Biol. 7:214.

Dufresne, E. R., H. Noh, V. Saranathan, S. G. J. Mochrie, H. Cao, and R. O. Prum. 2009. Self-assembly of amorphous biophotonic nanostructures by phase separation. Soft Matter 5:1792–1795.

Durrer, H. 1977. Schillerfarben der vogelfeder als evolutionsproblem. Denkschr. Schweiz. Naturf. Ges. 91:1–127.

Eliason, C. M., and M. D. Shawkey. 2012. A photonic heterostructure produces diverse iridescent colours in duck wing patches. J. R. Soc. Interface 9:2279–2289.

Emlen, D. J., J. Marangelo, B. Ball, and C. W. Cunningham. 2005. Diversity in the weapons of sexual selection: horn evolution in the beetle genus *Onthophagus* (Coleoptera: Scarabaeidae). Evolution 59:1060–1084.

Emlen, D. J., L. Corley Lavine, and B. Ewen-Campen. 2007. On the origin and evolutionary diversification of beetle horns. Proc. Natl. Acad. Sci. 104 (Suppl 1):8661–8668.

Figuerola, J., and A. Green. 2000. The evolution of sexual dimorphism in relation to mating patterns, cavity nesting, insularity and sympatry in the Anseriformes. Funct. Ecol. 14:701–710.

Gill, F., and D. Donsker (eds). 2014. IOC world bird list (v 4.4). Available at http://www.worldbirdnames.org. doi: 10.14344/IOC.ML.4.4.

Gingerich, P. D. 2009. Rates of evolution. Annu. Rev. Ecol. Evol. Syst. 40:657–675.

Gonzalez, J., H. Düttmann, and M. Wink. 2009. Phylogenetic relationships based on two mitochondrial genes and hybridization patterns in Anatidae. J. Zool. 279:310–318.

Greenewalt, C., W. Brandt, and D. Friel. 1960. Iridescent colors of hummingbird feathers. J. Opt. Soc. Am. 50:1005–1013.

Hansen, T. 1997. Stabilizing selection and the comparative analysis of adaptation. Evolution 51:1341–1351.

Hansen, T. F., and E. P. Martins. 1996. Translating between microevolutionary process and macroevolutionary patterns: the correlation structure of interspecific data. Evolution 50:1404–1417.

Harmon, L. J., and J. B. Losos. 2005. The effect of intraspecific sample size on type I and type II error rates in comparative studies. Evolution 59:2705–2710.

Harmon, L. J., J. B. Losos, T. Jonathan Davies, R. G. Gillespie, J. L. Gittleman, W. Bryan Jennings, K. H. Kozak, M. A. McPeek, F. Moreno-Roark, T. J. Near, et al. 2010. Early bursts of body size and shape evolution are rare in comparative data. Evolution 64:2385–2396.

Hill, G. E. 2006. Female mate choice for ornamental coloration. Pp. 137–200 *in* K. J. McGraw and G. E. Hill, eds. Bird coloration: volume II. Harvard Univ. Press, Cambridge, MA.

Hoekstra, H. E., J. M. Hoekstra, D. Berrigan, S. N. Vignieri, A. Hoang, C. E. Hill, P. Beerli, and J. G. Kingsolver. 2001. Strength and tempo of directional selection in the wild. Proc. Natl. Acad. Sci. 98:9157–9160.

Holm, S. 1979. A simple sequentially rejective multiple test procedure. Scand. J. Stat. 6:65–70.

Holzman, R., D. C. Collar, R. S. Mehta, and P. C. Wainwright. 2011. Functional complexity can mitigate performance trade-offs. Am. Nat. 177:E69–E83.

Huelsenbeck, J. P., and F. Ronquist. 2001. MRBAYES: Bayesian inference of phylogenetic trees. Bioinformatics 17:754–755.

Hulsey, C. D. C., F. J. F. G. de León, and R. R. Rodiles-Hernández. 2006. Micro- and macroevolutionary decoupling of cichlid jaws: a test of Liem's key innovation hypothesis. Evolution 60:2096–2109.

Hunt, G. 2012. Measuring rates of phenotypic evolution and the inseparability of tempo and mode. Paleobiology 38:351–373.

Ives, A. R., P. E. Midford, and T. Garland Jr. 2007. Within-species variation and measurement error in phylogenetic comparative methods. Syst. Biol. 56:252–270.

Joannopoulos, J. D., S. G. Johnson, J. N. Winn, and R. D. Meade. 2008. Photonic crystals: molding the flow of light. Princeton Univ. Press, Princeton, NJ.

Johnson, K. P., and M. D. Sorenson. 1999. Phylogeny and biogeography of dabbling ducks (genus: *Anas*): a comparison of molecular and morphological evidence. The Auk 116:792–805.

Kingsolver, J. G., and M. Koehl. 1994. Selective factors in the evolution of insect wings. Annu. Rev. Entomol. 39:425–451.

Kinoshita, S. 2008. Structural colors in the realm of nature. World Scientific, Singapore.

Klingenberg, C. P. 2008. Morphological integration and developmental modularity. Annu. Rev. Ecol. Evol. Syst. 39:115–132.

Legagneux, P., M. Théry, M. Guillemain, D. Gomez, and V. Bretagnolle. 2010. Condition dependence of iridescent wing flash-marks in two species of dabbling ducks. Behav. Process. 83:324–330.

Li, Q., K.-Q. Gao, Q. Meng, J. A. Clarke, M. D. Shawkey, L. D'Alba, R. Pei, M. Ellison, M. A. Norell, and J. Vinther. 2012. Reconstruction of microraptor and the evolution of iridescent plumage. Science 335:1215–1219.

Madge, S., and H. Burn. 1988. Wildfowl: an identification guide to the ducks, geese and swans of the world. A&C Black, Lond.

Maia, R., C. M. Eliason, P.-P. Bitton, S. M. Doucet, and M. D. Shawkey. 2013a. pavo: an R package for the analysis, visualization and organization of spectral data. Methods Ecol. Evol. 4:906–913.

Maia, R., D. R. Rubenstein, and M. D. Shawkey. 2013b. Key ornamental innovations facilitate diversification in an avian radiation. Proc. Natl. Acad. Sci. 110:10687–10692.

Maia, R., R. H. F. Macedo, and M. D. Shawkey. 2012. Nanostructural self-assembly of iridescent feather barbules through depletion attraction of melanosomes during keratinization. J. R. Soc. Interface 9:734–743.

Marks, M., and M. Seabra. 2001. The melanosome: Membrane dynamics in black and white. Nat. Rev. Mol. Cell. Bio. 2:738–748.

Martins, E. P. 1994. Estimating the rate of phenotypic evolution from comparative data. Am. Nat. 144:193–209.

Martins, E. P., J. A. F. Diniz-Filho, and E. A. Housworth. 2002. Adaptive constraints and the phylogenetic comparative method: a computer simulation test. Evolution 56:1–13.

Meadows, M. G., N. I. Morehouse, R. L. Rutowski, J. M. Douglas, and K. J. Mcgraw. 2011. Quantifying iridescent coloration in animals: a method for improving repeatability. Behav. Ecol. Sociobiol. 65:1317–1327.

Newton, I. 1704. Opticks. Royal Society, Lond.

Omland, K. 1997. Examining two standard assumptions of ancestral reconstructions: repeated loss of dichromatism in dabbling ducks (Anatini). Evolution 51:1636–1646.

Omland, K. 1996. Female mallard mating preferences for multiple male ornaments. Behav. Ecol. Sociobiol. 39:353–360.

Ord, T. J., D. C. Collar, and T. J. Sanger. 2013. The biomechanical basis of evolutionary change in a territorial display. Funct. Ecol. 27:1186–1200.

Orfanidis, S. 2008. Electromagnetic waves and antennas. Available at http://www.ece.rutgers.edu/~orfanidi/ewa/. Accessed July 1, 2014.

Paradis, E., J. Claude, and K. Strimmer. 2004. APE: analyses of phylogenetics and evolution in R language. Bioinformatics 20:289–290.

Paradis, E. J. 2012. Analysis of phylogenetics and evolution with R. 2nd ed. Springer, New York, NY.

Pigliucci, M. 2008. Is evolvability evolvable? Nat. Rev. Genet. 9:75–82.

Podos, J. 1997. A performance constraint on the evolution of trilled vocalizations in a songbird family (Passeriformes: Emberizidae). Evolution 51:537–551.

Prum, R. O. 2006. Anatomy, physics, and evolution of structural colors. Pp. 295–353 *in* K. J. McGraw and G. E. Hill, eds. Bird coloration, Vol. I. Harvard Univ. Press, Cambridge, MA.

Prum, R. O. 2010. The Lande–Kirkpatrick mechanism is the null model of evolution by intersexual selection: implications for meaning, honesty, and design in intersexual signals. Evolution 64:3085–3100.

Prum, R. O., and J. Dyck. 2003. A hierarchical model of plumage: morphology, development, and evolution. J. Exp. Zool. B Mol. Dev. Evol. 298: 73–90.

R Development Core Team. 2013. R: a language and environment for statistical computing. R Foundation for Statistical Computing, Vienna, Austria.

Rengarajan, R., D. Mittleman, C. Rich, and V. Colvin. 2005. Effect of disorder on the optical properties of colloidal crystals. Phys. Rev. E. 71:016615.

Ritchie, M. G. 2007. Sexual selection and speciation. Annu. Rev. Ecol. Evol. Syst. 38:79–102.

Rodríguez, R. L., J. W. Boughman, D. A. Gray, E. A. Hebets, G. Höbel, and L. B. Symes. 2013. Diversification under sexual selection: the relative roles of mate preference strength and the degree of divergence in mate preferences. Ecol. Lett. 16:964–974.

Safran, R. J., and K. J. Mcgraw. 2004. Plumage coloration, not length or symmetry of tail-streamers, is a sexually selected trait in North American barn swallows. Behav. Ecol. 15:455–461.

Schaeffer, B., and D. E. Rosen. 1961. Major adaptive levels in the evolution of the actinopterygian feeding mechanism. Am. Zool. 1:187–204.

Schielzeth, H. 2010. Simple means to improve the interpretability of regression coefficients. Methods Ecol. Evol. 1:103–113.

Schwenk, K., D. K. Padilla, G. S. Bakken, and R. J. Full. 2009. Grand challenges in organismal biology. Integr. Comp. Biol. 49:7–14.

Shawkey, M. D., M. E. Hauber, L. K. Estep, and G. E. Hill. 2006. Evolutionary transitions and mechanisms of matte and iridescent plumage coloration in grackles and allies (Icteridae). J. R. Soc. Interface 3:777–786.

Slater, G. J. 2013. Phylogenetic evidence for a shift in the mode of mammalian body size evolution at the Cretaceous-Palaeogene boundary. Methods Ecol. Evol. 4:734–744.

Sorenson, L. G., and S. R. Derrickson. 1994. Sexual selection in the northern pintail (*Anas acuta*): the importance of female choice versus male-male competition in the evolution of sexually-selected traits. Behav. Ecol. Sociobiol. 35:389–400.

Stayton, C. T. 2006. Testing hypotheses of convergence with multivariate data: morphological and functional convergence among herbivorous lizards. Evolution 60:824–841.

Wagner, G. P., M. Pavlicev, and J. M. Cheverud. 2007. The road to modularity. Nat. Rev. Genet. 8:921–931.

Wainwright, P. C. 2007. Functional versus morphological diversity in macroevolution. Annu. Rev. Ecol. Evol. Syst. 38:381–401.

Walker, J. A. 2007. A general model of functional constraints on phenotypic evolution. Am. Nat. 170:681–689.

West-Eberhard, M. J. 1983. Sexual selection, social competition, and speciation. Quart. Rev. Biol. 58:155–183.

Wund, M. A. 2012. Assessing the impacts of phenotypic plasticity on evolution. Integr. Comp. Biol. 52:5–15.

Xiao, M., A. Dhinojwala, and M. Shawkey. 2014. Nanostructural basis of rainbow-like iridescence in common bronzewing Phaps chalcoptera feathers. Opt. Express 22:14625–14636.

Associate Editor: M. Alfaro
Handling Editor: R. Shaw

Supporting Information

Additional Supporting Information may be found in the online version of this article at the publisher's website:

Table S1. Feather specimen museum locations and sample sizes for each species.
Table S2. Fossil data used for setting node constraints in BEAST.
Table S3. Comparison between intra- and interspecific trait variation in ducks.
Figure S1. Rarefaction of variance plots for diagonal and off-diagonal evolutionary variance-covariance matrix for nanostructural variables.
Figure S2. Rarefaction of variance plots for diagonal and off-diagonal components of the evolutionary variance-covariance matrix for color variables.
Figure S3. Patterns of covariation in color variables of duck wing feathers.
Figure S4. Patterns of morphological covariation in nanostructural traits within dabbling duck feathers.
Figure S5. Calibrated maximum clade credibility (MCC) tree for dabbling ducks (tribe Anatini).
Figure S6. Selecting the best evolutionary model.
Figure S7. Measurement error effects on evolutionary rates of nanostructural (A) and optical traits (B) in ducks.
Figure S8. Measurement error effects on evolutionary correlations of nanostructural (A) and optical traits (B) in ducks.
Figure S9. Modularity and rates of evolution for measured and predicted color variables.
Figure S10. Boxplots (left panels) show distribution of parameter values for α (red) and σ^2 (blue) in functionally related morphological (A) and optical traits (B).